

Novel enzymatic synthesis of spacer-linked Pk trisaccharide targeting for neutralization of Shiga toxin

著者	Kato Tatsuya, Oizumi Takahiro, Ogata Makoto, Murakawa Akiko, Usui Taichi, Park Enoch Y.
journal or publication title	Journal of Biotechnology
volume	209
page range	50-57
year	2015-09-10
出版者	Elsevier
権利	Copyright (C) 2015 Elsevier B.V. All rights reserved.
URL	http://hdl.handle.net/10297/9723

doi: 10.1016/j.jbiotec.2015.06.403

1 Novel enzymatic synthesis of spacer-linked P^k trisaccharide
2 targeting for neutralization of Shiga toxin

3

4 Tatsuya Kato^{a,b,c}, Takahiro Oizumi^a, Makoto Ogata^d, Akiko Murakawa^c, Taichi Usui^c,
5 Enoch Y. Park^{a,b,c*}

6

7 ^a *Laboratory of Biotechnology, Department of Applied Biological Chemistry, Faculty of*
8 *Agriculture, Shizuoka University, 836 Ohya, Suruga-ku, Shizuoka 422-8529, Japan*

9 ^b *Laboratory of Biotechnology, Green Chemistry Research Division, Research Institute*
10 *of Green Science and Technology, Shizuoka University, 836 Ohya Suruga-ku, Shizuoka*
11 *422-8529, Japan*

12 ^c *Laboratory of Biotechnology, Integrated Bioscience Section, Graduate School of*
13 *Science and Technology, Shizuoka University, 836 Ohya, Suruga-ku, Shizuoka, 422-*
14 *8529, Japan*

15 ^d *Department of Chemistry and Biochemistry, Fukushima National College of*
16 *Technology, 30 Nagao, Iwaki, Fukushima 970-8034 Japan*

17

* Corresponding author at: Green Chemistry Research Division, Research Institute of Green Science and Technology, Shizuoka University, 836 Ohya Suruga-ku, Shizuoka 422-8529, Japan. Tel. & Fax: +81 54 238 4887. E-mail address: acypark@ipc.shizuoka.ac.jp (Enoch Y. Park).

18 **ABSTRACT**

19 A novel alkyl spacer-conjugated derivative of P^k trisaccharide (P^k), one of the active
20 receptors of Shiga toxins (Stxs; Stx1 and Stx2) produced by pathogenic *Escherichia*
21 *coli* (STEC), was designed and synthesized by a combination of cellulase-mediated
22 condensation from *Trichoderma reesei* and α1,4-galactosyltransferase (LgtC) from
23 *Neisseria gonorrhoeae*. The specific activity of *N. gonorrhoeae* LgtC was 66 U/mg,
24 which was 13-fold higher than that from *N. meningitidis* expressed in *E. coli*. 5-
25 Trifluoroacetamidopentyl-β-P^k (TFAP-P^k) was synthesized (yield of 86%, based on the
26 amount of TFAP-lactose added) and its binding to Stx1a-B and Stx2a-B was evaluated.
27 The dissociation constants (K_{Ds}) of Stx1a-B and Stx2a-B to the spacer-linked P^k,
28 immobilized on a CM5 sensor chip, were 6.8×10^{-6} M ($k_{on} = 4.1 \times 10^1$ M⁻¹S⁻¹, $k_{off} = 2.8$
29 $\times 10^{-4}$ S⁻¹) and 2.2×10^{-5} M ($k_{on} = 3.9 \times 10^2$ M⁻¹S⁻¹, $k_{off} = 8.6 \times 10^{-3}$ S⁻¹), respectively.
30 This result suggests that the monovalent P^k-derivative, conjugated to a pentylamino
31 group, represents a promising Stx-neutralizing agent. This cellulase-mediated
32 condensation using cellulase and glycosyltransferase is a valuable tool for the synthesis
33 of spacer-linked oligosaccharide.

34 **Keywords:** α1,4-Galactosyltransferase; Shiga toxin; Globotriose; *Neisseria*
35 *gonorrhoeae*; Cellulase-mediated condensation

36

37 **1. Introduction**

38 Cell surface glycans are involved in many physiological phenomena, including
39 cell differentiation, cell development, signal transduction, virus and pathogen infection,
40 and cancer metastasis. Glycan-binding proteins (GBPs) have crucial roles in these
41 phenomena by recognizing and binding specific glycans. This GBP-glycan interaction
42 is comparatively weak, compared to protein-protein interactions, but is never
43 negligible biologically, because glycans are very important molecules together with
44 proteins and nucleic acids (van Kooyk and Rabinovich, 2008). In addition, synthetic
45 glycans and oligosaccharides have been investigated for the detection and prevention
46 of virus infection (Ogata et al., 2007; Schofield et al., 2007).

47 To analyze the binding properties of GBPs, various glycan arrays have now been
48 developed, in which chemically synthesized glycans containing an amine or other
49 functional group are arrayed on *N*-hydroxysuccinimide (NHS)- or epoxy-activated
50 glass slides (Blixt et al., 2004). Such a glycan array was previously utilized as a glycan
51 library to investigate various GBP-binding parameters (Song et al., 2008). Several
52 glycans and oligosaccharides have been synthesized by chemical and enzymatic
53 reactions to investigate their characteristic properties and GBP specificity (Hsu et al.,
54 2011; Lepenies et al., 2010). In chemical synthesis of glycan, many tedious steps
55 required to protect and deprotect hydroxyl groups (Pazynina et al., 2002; 2003) can be
56 circumvented by stereo- and region-specific reaction by glycosyltransferases (Palcic,
57 2011). From a practical point, the use of glycosyltransferases is attractive for glycan
58 synthesis, because it is highly regioselective for specific hydroxyl groups. On the other
59 hand, glycosidases, which normally hydrolyze glycosidic bonds, catalyze two types of

60 reactions, transglycosylation (Yamamoto, 2013) and condensation (Yasutake et al.,
61 2003), and the condensation reaction has been used in the synthesis of spacer-*O*-linked
62 glycans.

63 In the present study, a novel P^k trisaccharide (P^k)-conjugated derivative with an
64 alkyl spacer, a sugar unit monomer in the chemical structure, was designed and
65 synthesized by the combination of cellulase-mediated condensation, by *Trichoderma*
66 *reesei* glycosidase, and glycan transfer, using the *Neisseria gonorrhoeae* α1,4-
67 galactosyltransferase (LgtC). This P^k would be expected to bind *E. coli* O-157 Shiga-
68 like toxins 1a (Stx-1) and 2 (Stx-2). Shiga toxin-producing *E. coli* (STEC) produces
69 Shiga toxin (Stx), which belongs to the AB₅ family of protein toxins, composed of one
70 A subunit and five B subunits (Bergan et al., 2012). The A subunit has RNA *N*-
71 glycosidase activity that causes cell death by inhibiting protein synthesis. The B
72 subunit is non-toxic and functions to bind P^k to the surface of eukaryotic cells,
73 allowing the toxin to enter the cell. Each B subunit has three P^k-binding sites, thus
74 totaling 15 P^k binding sites per Stx molecule. We showed that this monovalent P^k-
75 derivative, conjugated with a pentylamino group, showed strong binding activity to
76 both Stx-1 and Stx-2, and thus represents a promising new candidate Stx-neutralizing
77 agent.

78 **2. Materials and methods**

79 *2.1. Expression of N. gonorrhoeae LgtC and Stxs B subunits*

80 A partially deleted *lgtC* gene (1–858 bp) of *N. gonorrhoeae* F62 was synthesized
81 by Eurofins MWG Operon (Tokyo, Japan). This synthesized *lgtC* gene was codon-

82 optimized for expression in *E. coli* with its C-terminal 25 amino acids deleted. To
83 attach a spacer (GGGGSGGGGS) and 6 × His tag, the *lgtC* gene was amplified by
84 PCR using A4GalT-frw and A4GalT-21-rev primers (Table 1). In addition, the
85 sequence of the spacer and 6 × His tag was prepared using GS-H6 as a PCR template
86 for GS-H6(-21)-frw and GS-H6-rev PCR primers. The *lgtC* gene attached to the spacer
87 and 6 × His tag was PCR-amplified using the *lgtC* gene and DNA fragment of the
88 spacer and 6 × His tag as templates and the A4GalT-frw and GS-H6-rev primers (Table
89 1). The amplified gene was then inserted into a pET32b vector by In-Fusion
90 technology (CLONTECH, Mountain View, CA, USA). Linearized pET32b was
91 prepared by PCR using pET32-frw and pET32-rev as primers. The recombinant
92 pET32b construct was transformed into *E. coli* BL21 (DE3) cells. Expression of 6 ×
93 His-tagged LgtC was induced by the addition of 1 mM isopropyl-β-D-1-
94 thiogalactopyranoside (IPTG) in the culture of this transformant in LB medium
95 supplemented with 100 μg/ml of ampicillin.

96 DNA fragments composed of the coding sequences for the Stx1a-B and Stx2a-B
97 subunits were synthesized by Eurofins MWG Operon, Inc. To attach the sequence of a
98 spacer (GGGGSGGGGS) and 6 × His tag, each B subunit gene was amplified by PCR
99 using Stx1a-B-frw and Stx1a-B-rev primers or Stx2a-B-frw and Stx2a-B-rev primers
100 (Table 1), respectively. The sequence of the spacer and 6 × His tag was also prepared
101 using GS-H6 as a PCR template and GS-H6-1aB-frw or GS-H6-2aB-frw and GS-H6-
102 rev as PCR primers. The sequence containing the spacer and 6 × His tag was added to
103 each gene by PCR, and the amplified genes inserted into pET32b vectors in the same
104 manner as the *lgtC-His* gene, using In-Fusion technology. Each constructed vector was
105 then transformed into *E. coli* BL21 (DE3) cells, and the expression of each His-tagged

106 B subunit carried out in the same manner as LgtC expression.

107 2.2. Purification of LgtC and Stx B subunits

108 Purification of LgtC, Stx1a-B-His and Stx2a-B-His was performed using His60 Ni
109 Super flow (CLONTECH) or TALON affinity gel column chromatography. Pelleted
110 cells were suspended in 50 mM Tris-HCl (pH 7.8) containing 150 mM NaCl (Buffer A)
111 and disrupted by sonication. The homogenate was then centrifuged at $5000 \times g$ and the
112 supernatant collected and loaded onto a TALON resin affinity column, and this column
113 was washed by Buffer A containing 40 mM imidazole. Each protein was eluted with
114 Buffer A containing 300 mM imidazole. For size-exclusion chromatography, a
115 Superdex 200 10/300 GL column (GE Healthcare Japan, Tokyo, Japan) was used.
116 Buffer A was used as a running buffer. One milliliter of purified Stx1a-B (0.05 mg/ml)
117 or Stx2a-B (0.4 mg/ml) was used for this size-exclusion chromatography.

118 2.3. SDS-PAGE

119 Recombinant protein samples were subjected to SDS-PAGE on 10 or 12%
120 polyacrylamide gels using the Mini-protean II system (Bio-Rad, Hercules, CA, USA).
121 For Stx-Bs, Tris-Tricine SDS-PAGE was adopted. Total proteins on SDS-PAGE gels
122 were detected by Coomassie Brilliant blue R-250 or silver staining. Protein
123 concentrations were measured by BCA Protein Assay-Reducing Agent Compatible
124 (Thermo Fisher Scientific, Rockford, IL, USA).

125 2.4. 5-Trifluoroacetamido-1-pentanol (TFAP)-linked P^k (TFAP- P^k) synthesis

126 Synthesis of TFAP- P^k was carried out according to the scheme in Fig. 1. 5-

127 Trifluoroacetamidopentyl β -lactoside (TFAP-Lac) was prepared by a protocol
128 described previously (Ogata et al., 2007). TFAP-Lac (40 mg, 0.076 mmol) and UDP-
129 Gal (94 mg, 0.15 mmol) were first dissolved in a solution that contained 10.3 ml of 50
130 mM Tris-HCl (pH 6.8), MnCl₂ (34.6 mg), and BSA (15.3 mg), and 15.5 U (5 ml) of
131 purified LgtC was then added. The mixture was then incubated for 4 h at 37°C, and the
132 reaction terminated by boiling for 5 min. The supernatant was isolated by
133 centrifugation (8000 \times g, 20 min), concentrated and dissolved in 5 ml of
134 CHCl₃/CH₃OH/H₂O (6:4:1), and loaded onto a Silica Gel 60 N column (4.5 \times 30 cm).
135 The same solvent at a flow rate of 10 ml/min was used as a running buffer and fraction
136 sizes of 20 ml/tube. Aliquots from fractions 17–26 were then concentrated, dissolved in
137 2 ml of 20% methanol, and loaded onto an ODS column (2.5 \times 30 cm) equilibrated
138 with 20% methanol, at a flow rate of 2.0 ml/min. After washing the column with 280
139 ml of 20% methanol, the absorbed material was eluted with 40% methanol and a
140 fraction size of 10 ml. The absorbance of the eluate was monitored at 210 nm. An
141 aliquot from pooled fractions 3–4 was concentrated by evaporation and lyophilized.
142 High resolution electrospray ionization mass spectrometry (HR-ESI-MS): m/z
143 708.23174 [M+Na]⁺ (calcd for C₂₅H₄₂F₃N₁NaO₁₇, 708.23025); ¹H NMR (D₂O, 500
144 MHz): δ 4.84 (d, 1H, $J_{1'',2''}$ 4.0 Hz, H-1''), 4.40 (d, 1H, $J_{1',2'}$ 8.0 Hz, H-1'), 4.37 (d, 1H,
145 $J_{1,2}$ 8.0 Hz, H-1), 4.25 (1H, H-5''), 3.93-3.45 (18H), 3.23 (2H, H- ϵ), 3.19 (1H, H-2),
146 1.55 (2H, H- β), 1.51 (2H, H- δ), 1.30 (2H, H- γ); ¹³C NMR (D₂O, 125 MHz): δ 158.9
147 (CF₃CONH-), 116.0 (CF₃CONH-), 103.3 (C-1'), 102.0 (C-1), 100.4 (C-1''), 78.8 (C-4),
148 77.4 (C-4'), 75.5 (C-5'), 74.9 (C-5), 74.6 (C-3), 73.0 (C-2), 72.2 (C-3'), 71.0 (C-5''),
149 70.9 (C-2'), 70.4 (C- α), 69.2 (C-3''), 69.0 (C-4''), 68.6 (C-2''), 60.6 (C-6''), 60.4 (C-6'),

150 60.1 (C-6), 39.7 (C-ε), 28.3 (C-β), 27.5 (C-δ), and 27.5 (C-γ).

151 2.5. Surface plasmon resonance (SPR)

152 SPR analyses were performed using Biacore 2000 (GE Healthcare Japan, Tokyo,
153 Japan). TFAP-P^k was treated with NaOH to remove trifluoroacetic acid (TFA) from
154 amino groups and neutralized with HCl. The P^k was then immobilized onto a CM5
155 sensor chip (GE Healthcare Japan) by amine coupling at pH 4.0 (1500 – 2000 RU).
156 Stx1a-B or Stx2a-B were then injected into the sensor chip in HBS-EP buffer (10 mM
157 HEPES, 150 mM NaCl, 3 mM EDTA, 0.005% Surfactant P-20 [GE Healthcare Japan],
158 pH 7.4) at 30 μl/min. As a regeneration buffer, 10 mM 5-aminopentyl β-P^k (AP-P^k)
159 treated with NaOH was used. Kinetics analysis was performed using 1:1 Langmuir
160 binding model using BIAevaluation software (GE Healthcare Japan).

161 2.6. Analytical methods

162 The α1,4-Galactosyltransferase (α1,4GalT) activity of LgtC was assayed as
163 follows. UDP-galactose (UDP-Gal, gifted from Yamasa Corp, Chiba, Japan) (10 mM),
164 2-[5'-dimethylaminonaphthalene-1'-sulfonyl-(2-aminoethoxy)]ethyl β-lactoside
165 (dansyl-Lac, 5 mM), MnCl₂ (12.5 mM) and BSA (1 mg/ml) were dissolved in 50 mM
166 Tris-HCl (pH 6.8), followed by the addition of 100 μl of enzyme solution (total volume
167 286 μl). Dansyl-Lac was prepared as described previously (Ogata et al., 2010). The
168 reaction was initiated 37°C by addition of 100 μl enzyme solution (final concentration:
169 0.46 mg/ml of purified LgtC). At each sample time, 10 μl of the reaction mixture was
170 added to 190 μl distilled water, followed by immediate boiling for 5 min. After

171 filtration through a 0.45- μ m nitrocellulose filter (Millipore, Bedford, MA), the filtrates
172 were analyzed by HPLC (Jasco LC-2000, Jasco Ltd., Tokyo, Japan) plus fluorescence
173 detector (excitation, 330 nm; emission, 520 nm) (JOEL Ltd., Tokyo, Japan) using a
174 Unison US-C18 (ODS, 4.6 \times 250 mm, Imtakt, Japan) column, and eluted with 25%
175 acetonitrile. The HPLC was operated isocratically at a flow rate of 1.0 ml/min and a
176 column temperature of 40°C. One unit of enzyme activity was defined as the amount of
177 enzyme capable of catalyzing the transfer of 1 μ mol of Gal per minute.

178 Electro spray ionization (ESI) mass spectra were measured by a JMS-T100LC mass
179 spectrometer (JOEL). 500-MHz 1 H NMR spectra and 125-MHz 13 C NMR spectra were
180 recorded using a JNM-ECX500II spectrometer (JOEL). Chemical shifts were
181 expressed in ppm relative to the methyl resonance of the external standard sodium 3-
182 (trimethylsilyl) propionate.

183 **3. Results and discussion**

184 *3.1. Expression and purification of LgtC*

185 LgtC was expressed in the soluble fraction in *E. coli* and purified by His60 Ni
186 Super flow column chromatography with 300 mM imidazole. Purified LgtC was
187 observed as a single band on an SDS-PAGE gel (Fig. 2A), corresponding to its
188 molecular weight estimated from its amino acid sequence. α 4GnT activity of LgtC was
189 detected using Dansyl-Lac and UDP-Gal as substrate in both cell homogenates (Fig.
190 2B) and purified samples (Fig. 2C) also, indicating that active α 4GnT was expressed.
191 Expressed LgtC in *E. coli* was 13-fold purified from the crude extract and finally, 0.14

192 mg of purified LgtC was obtained from 100 ml *E. coli* culture (Table 2). The specific
193 activity of this purified LgtC was 66 U/mg, 13-fold higher than that of *N. meningitidis*
194 LgtC purified from *E. coli* (Zhang et al., 2002). In the study of *N. meningitidis* LgtC,
195 UDP-D-[6-³H] galactose and lactose were used for α 4GnT assay as a sugar donor and
196 acceptor, different from the substrates used in this study. This difference may cause
197 discrepancies between the specific activity of the *N. gonorrhoeae* LgtC (used here) and
198 that of *N. meningitidis* LgtC. Optimal pH and temperature in this assay were 8.0 and
199 40°C, respectively (Fig. 3).

200 3.2. TFAP- P^k synthesis

201 A condensation reaction between lactose and TFAP was first catalyzed by cellulase
202 from *T. reesei* to obtain TFAP-Lac, as described in our previous report (Ogata et al.,
203 2007). In this study, TFAP-lactose was obtained in 0.67% yield based on the initial
204 amount of lactose. This yield was a little lower than that (1.0%) in previous paper
205 (Ogata et al., 2007). The efficiency of this condensation reaction by cellulase is low,
206 but this reaction is an easy way to provide β -glycoside stereo-specifically, because it
207 does not require any protection and deprotection steps. A novel *O*-linked P^k -conjugated
208 derivative with an alkyl spacer was then derived from the resulting product utilizing
209 the above-described purified LgtC (Fig. 1). The yield of this reaction was 67% based
210 on the initial amount of TFAP-lactose. Addition of α 1,4-linked Gal to the TFAP-Lac
211 acceptor led to the synthesis of trisaccharide glycoside TFAP- P^k . Synthesized TFAP- P^k
212 was purified by Silica Gel 60 N column and ODS column (Fig. 4A) and HR-ESI-MS
213 analysis of synthesized TFAP- P^k showed $[M + Na^+]$ ion at m/z 708.23174,
214 corresponding to the molecular formula, C₂₅H₄₂F₃N₁NaO₁₇ (calcd, 708.23025) (Fig.

215 3B). In addition, ¹H NMR spectroscopy was performed to confirm the structure of
216 synthesized TFAP-P^k. LgtC purified from *E. coli* catalyzed the addition of galactose to
217 TFAP-N-acetyllactosamine (Fig. 5). In a previous study, lactosyl-ceramide was
218 galactosylated by catalytical reaction at the terminal Gal residue to obtain P^k-ceramide
219 using α4GalT from *N. meningitidis* (Adlercreutz et al., 2010). However, no additional
220 transfer of galactose to TFAP-P^k was observed here, using LgtC from *N. gonorrhoeae*
221 for a 4-h reaction, indicating that *N. gonorrhoeae* LgtC has more narrow substrate
222 specificity for P^k synthesis than α4GalT from *N. meningitidis*. In this point, LgtC from
223 *N. gonorrhoeae* is more feasible for P^k synthesis than α4GalT from *N. meningitidis*.

224 3.3. Expression and purification of Stxs B subunits

225 Stx1a-B and Stx2a-B were expressed in *E. coli* and purified using TALON affinity
226 gel chromatography. By SDS-PAGE, purified Stx1a-B and Stx2a-B were observed to
227 be close to their estimated molecular weights (Fig. 6A). MALDI-TOF MS revealed the
228 molecular weights of Stx1a-B and Stx2a-B to be 9139 Da and 8950 Da, respectively.
229 This result indicates that the native signal peptide of each B subunit was cleaved off
230 (1–20 aa of Stx1a-B and 1–19 aa of Stx2a-B), and each subunit might be secreted to
231 the periplasm. By SDS-PAGE, each protein band was observed to be over 10 kDa,
232 despite the exact molecular weight of both B subunits being below 10 kDa. This
233 discrepancy may be caused by the 6 × His tag slowing protein mobility through SDS-
234 PAGE, due to its positive charge. In gel filtration chromatography, each peak (Stx1a-B
235 and Stx2a-B) was observed at around 20 and 30 kDa (Fig. 6B), respectively, indicating
236 that these Stxs-B were expressed and purified as a dimer or trimer at 0.3 mM, and not
237 as a pentamer. In the range of 5 to 85 μM, recombinant Stx1a-B produced in *E. coli*

238 entirely formed pentamers, and recombinant Stx2a-B produced in *E. coli* existed
239 predominantly as pentamers at more than 50 μM (Kitova et al., 2005). In another
240 report, both recombinant subunits were expressed in *E. coli* as pentamers (Conrady et
241 al., 2010). In the current study, a $6 \times \text{His}$ tag was attached to the C-terminus of each B
242 subunit. These results suggest that the $6 \times \text{His}$ tag may prevent both B subunits from
243 forming pentamers.

244 3.4. P^k binding of Stx B subunits

245 The synthesized TFAP- P^k was deacylated to AP- P^k by alkali treatment. AP- P^k was
246 then immobilized on a CM5 chip by amine coupling, and various concentrations of
247 each B subunit were then applied to the CM5 chip. The K_D of each B subunit was
248 calculated by BIAevaluation software using obtained sensorgrams. Specific binding of
249 each B subunit was observed to TFAP- P^k immobilized on the CM5 chip (Fig. 7), and
250 each B subunit was washed out by free TFAP- P^k . The K_D s of Stx1a-B and Stx2a-B
251 were $6.8 \times 10^{-6} \text{ M}$ ($k_{on} = 4.1 \times 10^1 \text{ M}^{-1}\text{S}^{-1}$, $k_{off} = 2.8 \times 10^{-4} \text{ S}^{-1}$) and $2.2 \times 10^{-5} \text{ M}$ ($k_{on} =$
252 $3.9 \times 10^2 \text{ M}^{-1}\text{S}^{-1}$, $k_{off} = 8.6 \times 10^{-3} \text{ S}^{-1}$), respectively. Soltyk et al. reported that the K_D of
253 the Stx1 B subunit pentamer to P^k was $4.8 \times 10^{-3} \text{ M}$ when immobilized on a CM5
254 sensor chip, as determined by SPR (Soltyk et al., 2002). Here, SPR determinations of
255 k_{on} and k_{off} were impossible because the rapid kinetics of association and dissociation
256 of the P^k ligand was observed. However, the K_D of the same Stx1 B subunit pentamer
257 to P^k was previously reported to be $3 \times 10^{-9} \text{ M}$ ($k_{on} = 2 \times 10^5 \text{ M}^{-1}\text{S}^{-1}$, $k_{off} = 6 \times 10^{-4} \text{ S}^{-1}$)
258 when P^k incorporated into liposomes containing *Salmonella* serogroup B
259 lipopolysaccharide was immobilized on a CM5 sensor chip (Soltyk et al., 2002). Thus
260 theoretically, SPR in this study would be the same as the later experiment, in view of

261 the immobilization of P^k on the CM5 sensor chip, although the K_D of the Stx1 B
262 subunit pentamer in the previous paper (3×10^{-9} M) was >1000-fold smaller than that
263 of the Stx1a-B dimer used in this study (5.2×10^{-6} M). This difference might be caused
264 by the subunit state of Stx1a-B, pentamer or dimer. However, k_{off} of the B subunit
265 pentamer in the previous paper ($k_{off} = 6 \times 10^{-4}$ S⁻¹) is comparable to that of the Stx1a-B
266 dimer of this study ($k_{off} = 2.4 \times 10^{-4}$ S⁻¹), indicating that the subunit state of the Stx B
267 subunit is not involved in its dissociation from the P^k ligand but instead, has crucial
268 effects on its ligand association (k_{on}). The K_D of the Stx B subunit to P^k-Cer-displaying
269 cells was $10^{-8} - 10^{-9}$ M (Fuchs et al., 1986). These results showed that immobilization
270 of the P^k ligand on the sensor chip is favorable for kinetic analysis of the Stx B subunit,
271 and synthesis of the spacer-linked sugar chain is amenable to binding analysis of
272 glycan-binding proteins and further development of an Stx-neutralizing agent.
273 However, in this biacore analysis, 1:1 Langmuir binding model fitting was adopted in
274 spite of three P^k binding sites of Stx B subunits. 1:1 Langmuir binding model fitted the
275 sensorgrams with low value of χ^2 , 7.79 and 6.79 for Stx1 B subunit and Stx2 B
276 subunit, respectively. However this fitting model limits the detailed binding analysis of
277 the multivalency of Stx B subunits. If an isothermal titration calorimetry was used for
278 binding analysis of multivalency of Stx B subunits, highly accurate data would be
279 obtained.

280 In this study, we performed successfully novel enzymatic synthesis of spacer-
281 linked P^k trisaccharide (TFAP- P^k) by cellulose from *T. reesei* and recombinant LgtC of
282 *N. meningitides* purified from *E. coli*. The TFAP-P^k was utilized for the binding assay
283 of recombinant Stx B subunits to P^k by SPR experiment. This cellulase-mediated

284 condensation from cellulase and glycosyltransferase is a valuable tool for the synthesis
285 of spacer-linked oligosaccharide.

286 **Acknowledgement**

287 This work was supported partly by Promotion of Nanobio-Technology Research to
288 support Aging and Welfare Society from the Ministry of Education, Culture, Sports,
289 Science and Technology, Japan. There was no additional external funding received for
290 this study.

291 **References**

- 292 Adlercreutz, D., Weadge, J.T., Petersen, B.O., Duus, J.Ø., Dovichi, N.J., Palacic,
293 M.M., 2010. Enzymatic synthesis of Gb3 and iGb3 ceramides. *Carbohydrate*
294 *Research* 345, 1384–1388.
- 295 Bergan, J., Lingelem, A.B.D., Simm, R., Skotland, T., Sandvig, K., 2012. Shiga toxins.
296 *Toxicon* 60, 1085–1107.
- 297 Blixt, O., Head, S., Mondala, T., Scanlan, C., Hufletjt, M.E., Alvarez, R., Bryan, M.C.,
298 Fazio, F., Calarese, D., Stevens, J., Razi, N., Stevens, D.J., Skehel, J.J., van Die, I.,
299 Burton, D.R., Wilson, I.A., Cummings, R., Bovin, N., Wong, C.H., Paulson, J.C.,
300 2004. Printed covalent glycan array for ligand profiling of diverse glycan binding
301 proteins. *Proceedings of the National Academy Sciences USA* 101, 17033–17038.
- 302 Conrady, D.G., Flagler, M.J., Friedmann, D.R., vander Wielen, B.D., Kovall, R.A.,
303 Weiss, A.A., Herr, A.B., 2010. Molecular basis of differential B-pentamer stability
304 of Shiga toxins 1 and 2. *PLoS One* 5: e15153.

305 Fuchs, G., Mobassaleh, M., Donohue-Rolfe, A., Montgomery, R.K., Grand, R.J.,
306 Keusch, G.T., 1986. Pathogenesis of *Shigella diarrhea*: rabbit intestinal cell
307 microvillus membrane binding site for Shigella toxin. *Infection and Immunity* 53,
308 372–377.

309 Hsu, C.H., Hung, S.C., Wu, C.Y., Wong, C.H., 2011. Toward automated
310 oligosaccharide synthesis. *Angewandte Chemie- International Edition* 50, 11872–
311 11923.

312 Kitova, E.N., Daneshfar, R., Marcato, P., Mulvey, G.L., Armstrong, G., Klassen, J.S.,
313 2005. Stability of the homopentameric B subunits of Shiga toxins 1 and 2 in
314 solution and the gas phase as revealed by nanoelectrosprayfourier transform ion
315 cyclotron resonance mass spectrometry. *Journal of American Society of*
316 *Spectrometry* 16, 1957–1968.

317 Lepenies, B., Yin, J., Seeberger, P.H., 2010. Applications of synthetic carbohydrates to
318 chemical biology. *Current Opinion in Chemical Biology* 14, 404–411.

319 Ogata, M., Murata, T., Murakami, K., Suzuki, T., Hidari, K.I.P.J., Suzuki, Y., Usui, T.,
320 2007. Chemoenzymatic synthesis of artificial glycopolypeptides containing
321 multivalent sialyloligosaccharides with a γ -polyglutamic acid backbone and their
322 effect on inhibition of infection by influenza viruses. *Bioorganic Medicinal*
323 *Chemistry* 15, 1383–1393.

324 Ogata, M., Obara, T., Chuma, Y., Murata, T., Park, E.Y., Usui, T., 2010. Molecular
325 design of fluorescent labeled glycosides as acceptor substrates for
326 sialyltransferases. *Bioscience Biotechnology and Biochemistry* 74, 2287–2292.

327 Palcic, M.M., 2011. Glycosyltransferases as biocatalysts. *Current Opinion in Chemical*
328 *Biology* 15, 226–233.

329 Pazynina, G.V., Sablina, M.A., Tuzikov, A.B., Chinarev, A.A., Bovin, N., 2003.
330 Synthesis of complex α 2,3-sialooligosaccharides, including sulfated and
331 fucosylated ones, using Neu5Ac α 2-3Gal as a building block. *Mendeleev*
332 *Communications* 13, 245–248.

333 Pazynina, G.V., Severov, V.V., Bovin, N., 2002. Synthesis of N-acetylglucosamine-
334 terminated oligosaccharides-fragments of glycanprotein O-chains. *Mendeleev*
335 *Communications* 12, 183–184.

336 Schofield, C.L., Field, R.A., Russell, D.A., 2007. Glyconanoparticles for the
337 colorimetric detection of cholera toxin. *Analytical Chemistry* 79, 1356–1361.

338 Soltyk, A.M., MacKenzie, C.R., Wolski, V.M., Hiramata, T., Kitov, P.I., Bundle, D.R.,
339 Brunton, J.L., 2002. A mutational analysis of the globotriaosylceramide-binding
340 sites of verotoxin VT1. *Journal of Biological Chemistry* 277, 5351–5359.

341 Song, X., Xia, B., Lasanajak, Y., Smith, D.F., Cummings, R.D., 2008. Quantifiable
342 fluorescent glycan microarrays. *Glycoconjugate Journal* 25, 15–25.

343 van Kooyk, Y., Rabinovich, G.A., 2008. Protein-glycan interactions in the control of
344 innate and adaptive immune responses. *Nature Immunology* 9, 593–601.

345 Yamamoto, K., 2013. Recent advances in glycotecology for glycoconjugate
346 synthesis using microbial endoglycosidases. *Biotechnology Letters* 35, 1733–1743.

347 Yasutake, N., Totani, K., Harada, Y., Haraguchi, S., Murata, T., Usui, T., 2003.
348 Efficient synthesis of glycerol β -lactoside and its derivatives through a
349 condensation reaction by cellulase. *Biochimica et Biophysica Acta* 1620, 252–258.

350 Zhang, J., Kowal, P., Fang, J., Andreana, F., Wang, P.G., 2002. Efficient
351 chemoenzymatic synthesis of globotriose and its derivatives with a recombinant α -
352 (1 \rightarrow 4)-galactosyltransferase. *Carbohydrate Research* 337, 969–976.

353 **Table 1.** Primers and His-tag template.

Name	5' – 3'
A4GalT-frw	GAAGGAGATATACATGGACATCGTCTTTGCTGC
A4GalT-21-rev	GAGCCACCGCCACCCGGAGGAACAGCCAGTTTCC
GS-H6-(-21)-frw	GGAAACTGGCTGTTCCCTCCGGGTGGCGGTGGCTC
GS-H6-rev	CGCAAGCTTGTCGACTTAGTGGTGATGGTGATGATG
pET32-frw	ATGTATATCTCCTTCTTAAAGTTAAACAAAATTATTTC
pET32-rev	GTCGACAAGCTTGCGGC
Stx1a-B-frw	GAAGGAGATATACATGAAAAAACATTATTAATAGCTGC
Stx1a-B-rev	GAGCCACCGCCACCACGAAAAATAACTTCGCTGAATC
GS-H6-B1a-frw	GATTCAGCGAAGTATTTTTTCGTGGTGGCGGTGGCTC
Stx2a-B-frw	GAAGGAGATATACATGAAGAAGATGTTTATGGCGG
Stx2a-B-rev	GAGCCACCGCCACCGTCATTATTAAACTGCACTTCAGC
GS-H6-B2a-frw	GCTGAAGTGCAGTTTAATAATGACGGTGGCGGTGGCTC
GS-H6 template	GGTGGCGGTGGCTCTGGAGGCGGAGGCTCACATCATCACC ATCACCACTA

354

355 **Table 2.** Purification of recombinant LgtC.

	Volume (ml)	Activity (U)	Protein (mg)	Specific activity (U/mg)	Yield (%)	Purification (Fold)
Crude	2.5	52	11	5.0	100	1
Elution	2	9.3	0.14	66	18	13

356

357

358 **Figure legends**

359 **Fig. 1.** Scheme of enzymatic synthesis of TFAP-P^k.

360 **Fig. 2.** Purification and characterization of recombinant LgtC. (A) SDS-PAGE of
361 purified recombinant LgtC. Lane 1: molecular weight marker, lane 2: cell homogenate,
362 lane 3: purified LgtC. (B) HPLC chromatograms of LgtC reaction mixtures using cell
363 homogenate. (C) Time course of the production of Dansyl-P^k from Dansy-Lac using
364 purified recombinant LgtC.

365 **Fig. 3.** Characterization of recombinant LgtC. (A) Optimal pH of recombinant LgtC.
366 The activity was measured in each pH condition prepared by indicated buffers. (B)
367 Optimal temperature of recombinant LgtC. The assay was performed at each
368 temperature.

369 **Fig. 4.** Synthesis of TFAP-P^k. (A) Chromatogram of ODS column chromatography for
370 the purification of TFAP-P^k. TFAP-P^k was eluted by 40% methanol. (B) HR-ESI-MS
371 analysis of synthesized TFAP-P^k.

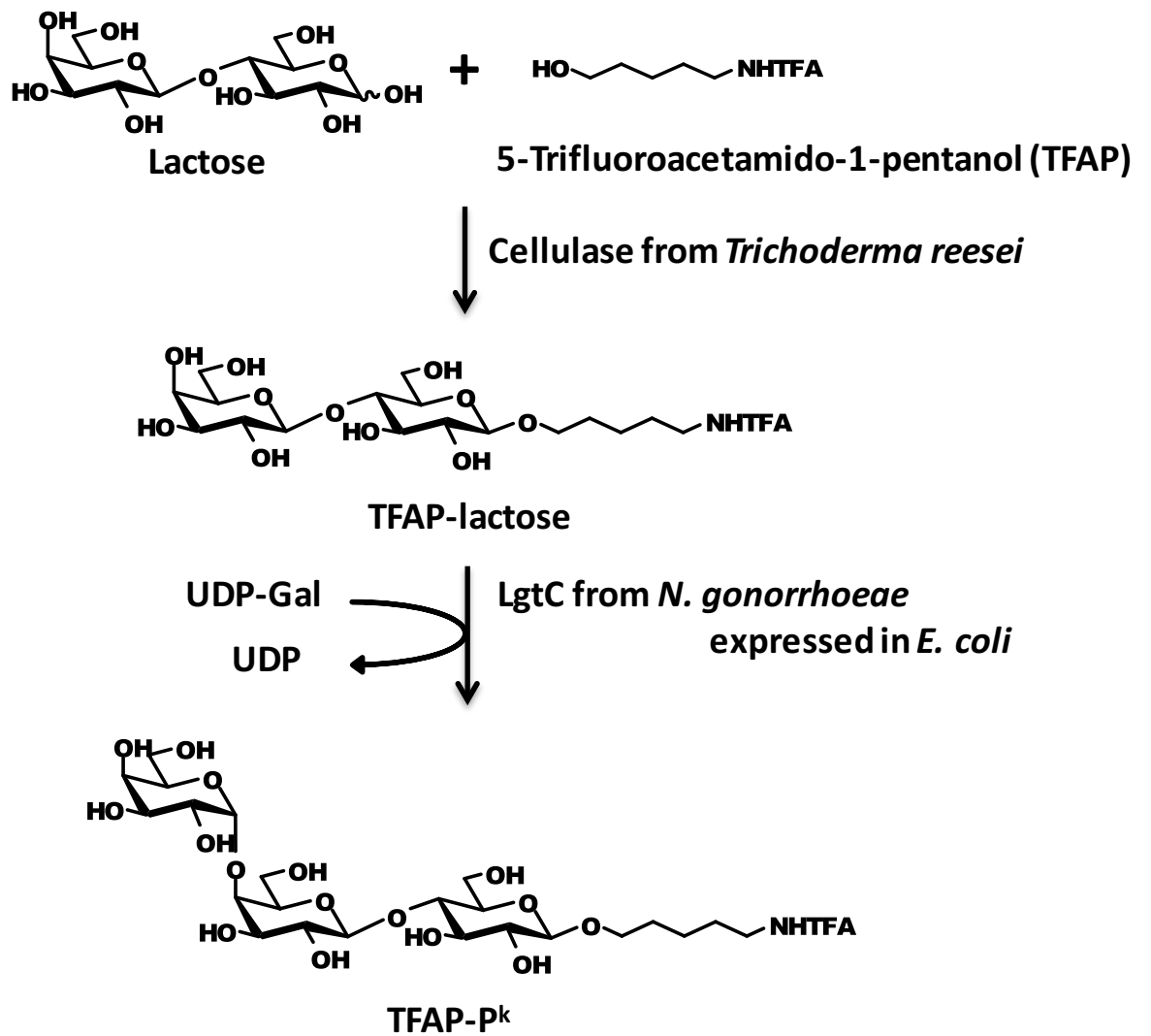
372 **Fig. 5.** 500 MHz ¹H NMR spectrum of TFAP-P^k. Solvent, D₂O; temperature, 25°C;
373 concentration, 8.3 mg/ml.

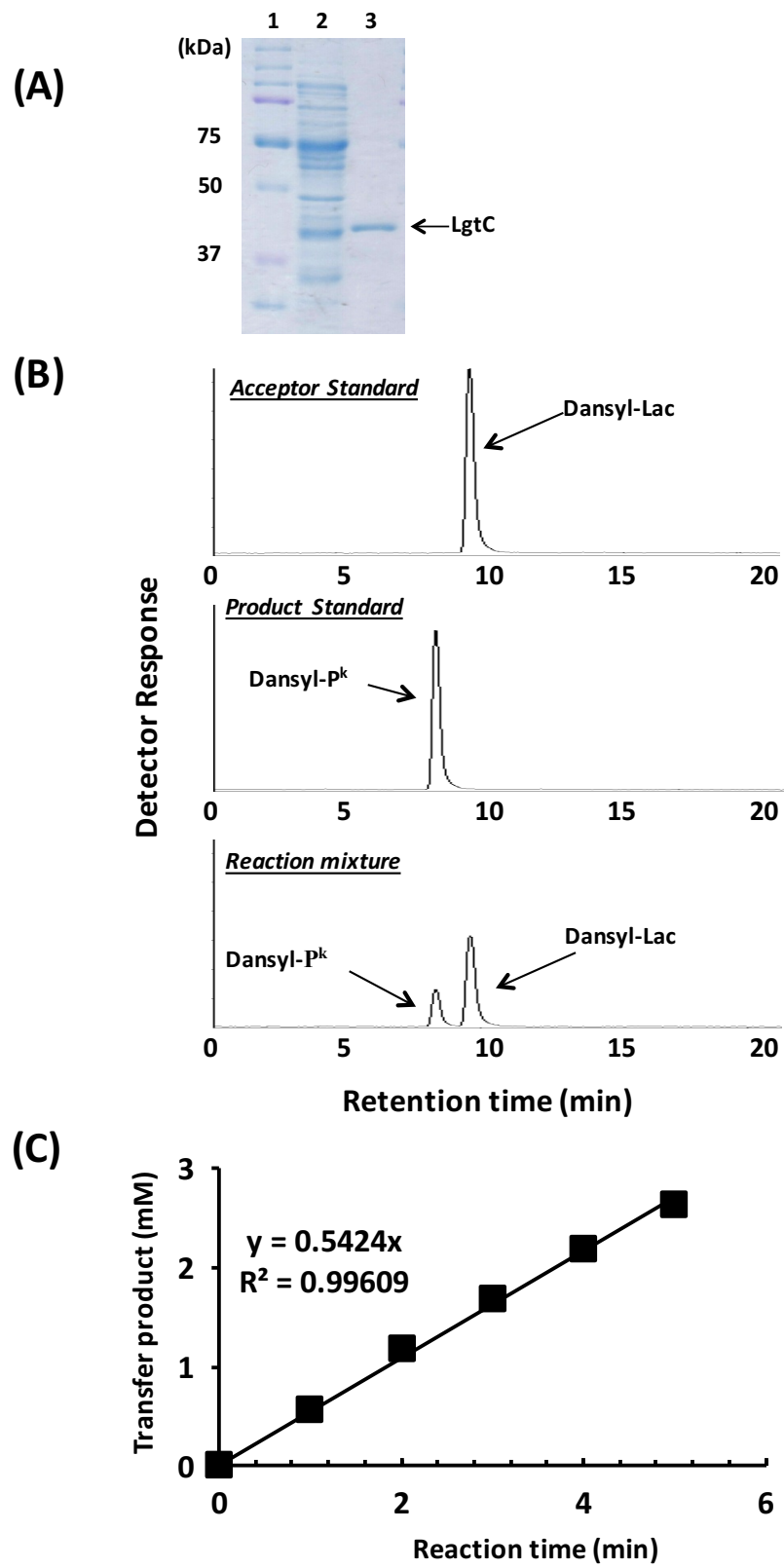
374 **Fig. 6.** Purification of recombinant Stx1a-B and Stx2a-B. (A) SDS-PAGE of Stx1a-B
375 and Stx2a-B purified by TALON affinity gel column chromatography. Lane 1:
376 molecular weight marker, lane 2: cell homogenate, Lane 3: wash fraction 1, lane 4:
377 wash fraction 2, lane 5: elution fraction. (B) Chromatograms of Superdex 200 10/300
378 GL column chromatography using one milliliter of purified Stx1a-B (0.05 mg/ml) and

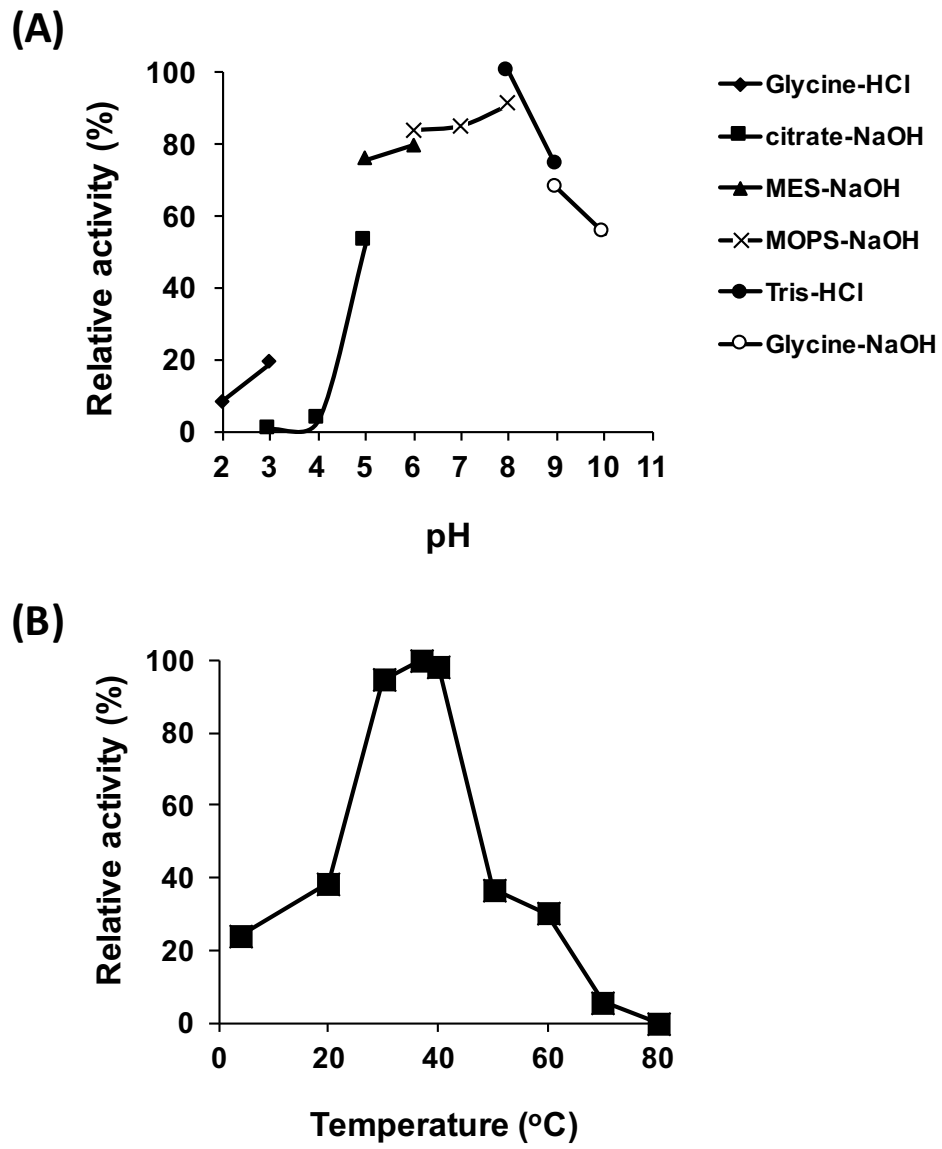
379 Stx2a-B (0.4 mg/ml). To estimate molecular weight of each purified protein, Gel
380 filtration calibration kit (Low molecular weight, GE Healthcare Japan) was used. This
381 kit contains Conalbumin (75 kDa), Ovalbumin (44 kDa), Carbonic anhydrase (29
382 kDa), Ribonuclease (13.7 kDa) and Aprotinin (6.5 kDa).

383 **Fig. 7.** Sensorgrams of SPR experiment using purified Stx1a-B and Stx2a-B. This SPR
384 experiment was performed using Biacore 2000. TFAP-P^k treated with NaOH was
385 immobilized on the CM5 sensor chip and each concentration of purified Stx1a-B or
386 Stx2a-B was injected into the sensor. As a regeneration buffer, 10 mM TFAP-P^k treated
387 with NaOH was used.

Figure 1, Kato et al.







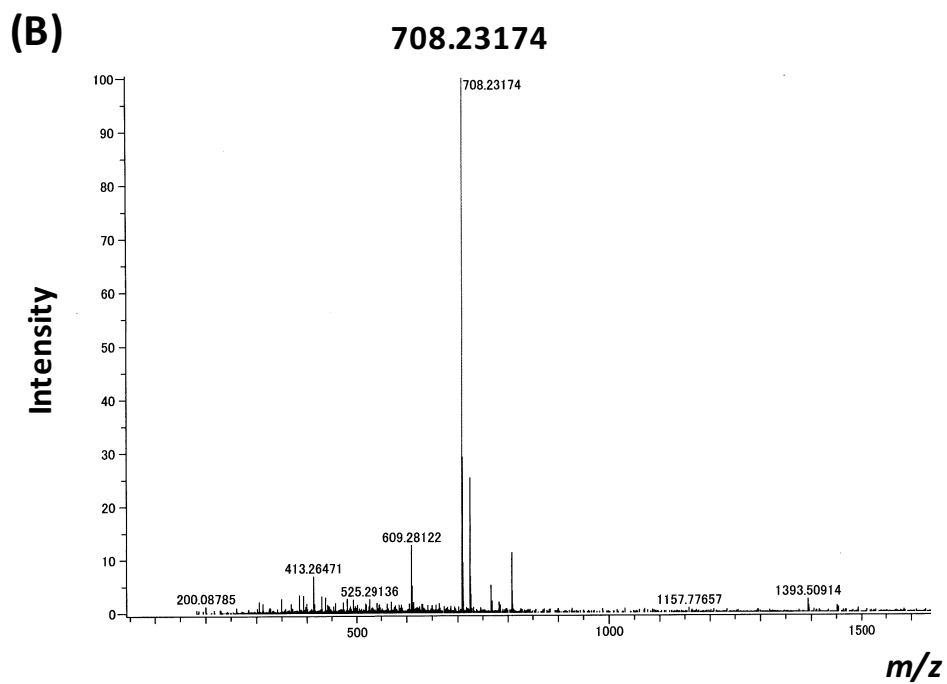
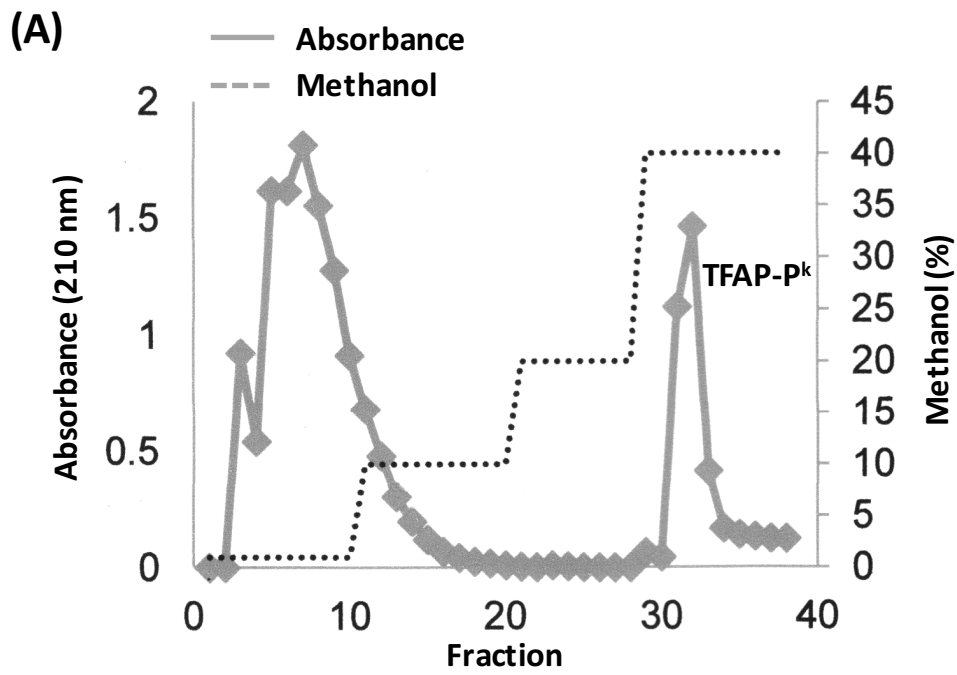


Figure 5, Kato et al.

